Supporting Information

Metal-ionic-conductor potassium ferrite nanocrystals with intrinsic superhydrophilic surface for electrocatalytic water splitting at ultrahigh current densities

Juan Jian,[#,a,c,] Wei Chen,[#,b,d] Decheng Zeng,[a] Limin Chang,[c] Ran Zhang,[d] Mingcheng Jiang,[a] Guangtao Yu,[*,b,d] Xuri Huang,[d] Hongming Yuan*[,a] and Shouhua Feng[a]

[a.] State Key Laboratory of Inorganic Synthesis and Preparative Chemistry, College of Chemistry, Jilin University, Changchun 130012, Qianjin Street 2699, P. R. China

[b.] Engineering Research Center of Industrial Biocatalysis, Fujian Province Higher Education Institutes, Fujian Provincial Key Laboratory of Advanced Materials Oriented Chemical Engineering, College of Chemistry and Material Science, Fujian Normal University, Fuzhou, 350007, China

[c.] Key Laboratory of Preparation and Applications of Environmental Friendly Material of the Ministry of Education, College of Chemistry, Jilin Normal University, Changchun 130103, P. R. China

[d.] Laboratory of Theoretical and Computational Chemistry, Institute of Theoretical Chemistry, Jilin University, Changchun 130023, P. R. China

Corresponding authors' E-mails: hmyuan@jlu.edu.cn; yugt@fjnu.edu.cn

Note: [#] authors made the same contribution to this article.

1. Materials and Corresponding Figures

1.1 Materials

RuO_2 is synthesized from ruthenium chloride hydrate ($RuCl_3 \cdot xH_2O$) purchased from Aladdin Ltd. (Shanghai, China).[1] Pt/C (20 wt%) is obtained from Macklin Ltd. (Shanghai, China), nickel foam (NF) is provided by the Li Yuan Technology Co. Ltd. (Shanxi, China). KOH, $Fe(NO_3)_3 \cdot 9H_2O$, HCl and other chemicals are supplied by the Beijing Chemical Reagents Company. All the chemicals are analytical pure and do not needed further purification.

1.2 Supplementary Figures

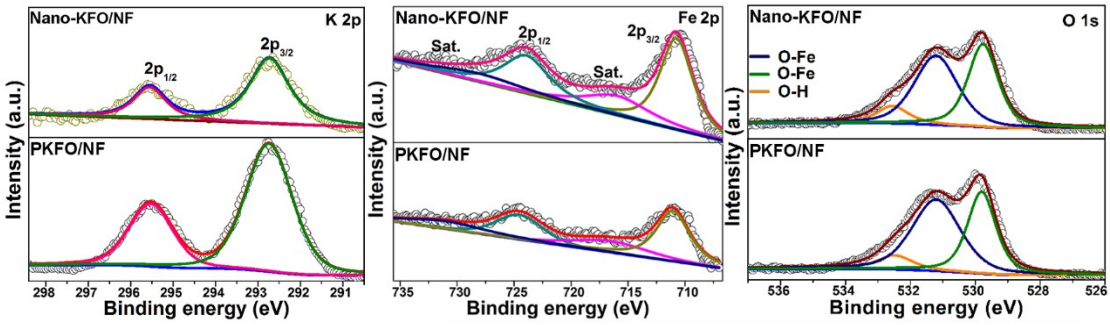

Fig. S1. The XPS results of (a) K 2p, (b) Fe 2p and (c) O 1s in Nano-KFO/NF and PKFO/NF, respectively.

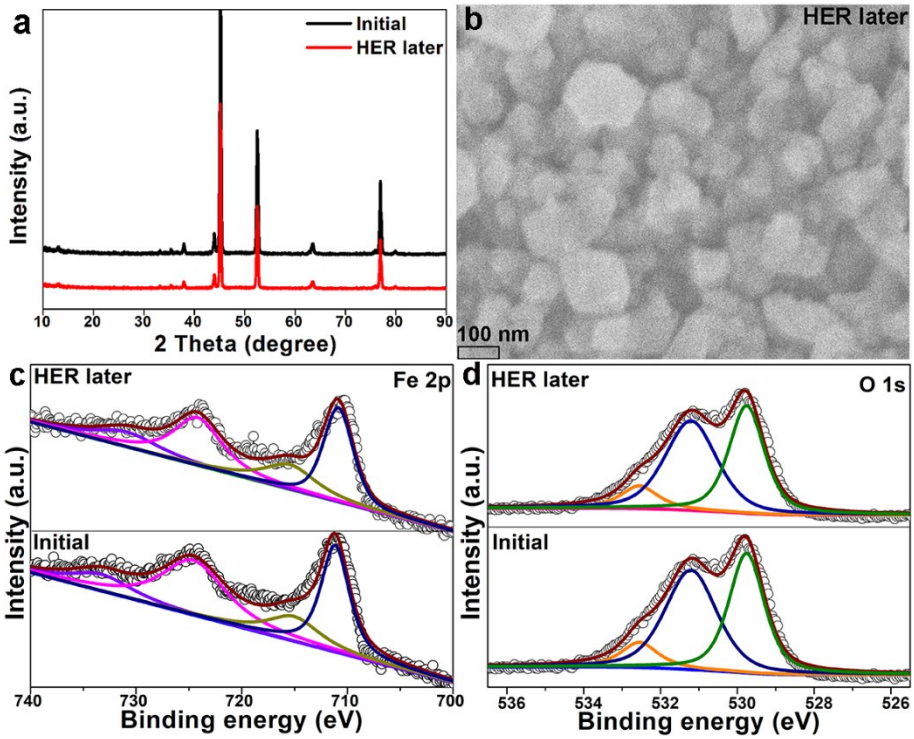

Fig. S2. The (a) XRD, (b) SEM results of Nano-KFO/NF after HER, and (c, d) the corresponding XPS results of Nano-KFO/NF that before and after the HER.

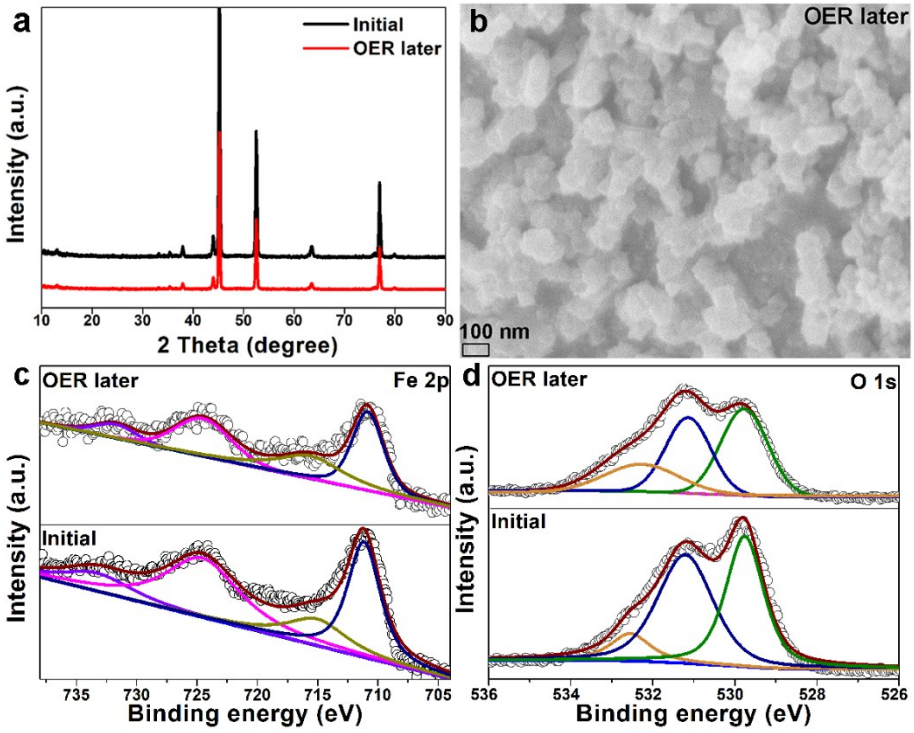

Fig. S3. The (a) XRD, (b) SEM results of Nano-KFO/NF after OER, and (c, d) the corresponding XPS results of Nano-KFO/NF that before and after the OER.

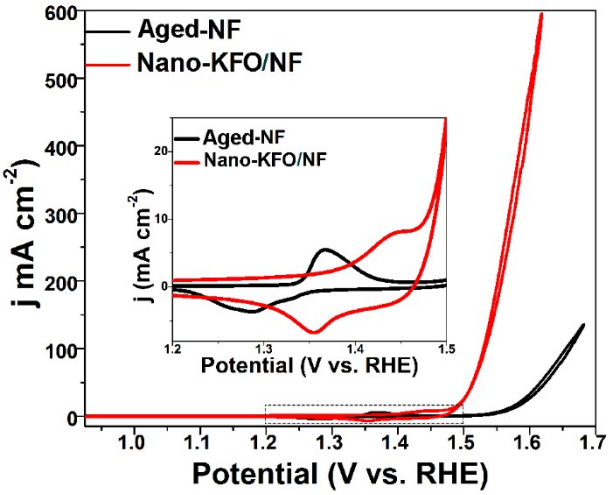

Fig. S4. The CV curves of Nano-KFO/NF and Aged-NF, illustration is an enlarged photo in the dotted box.

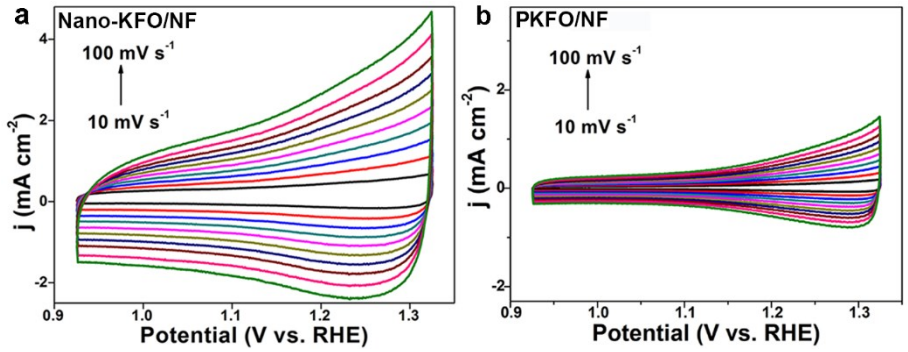

Fig. S5. The CV curves (in the range of non-Faraday potential) of the as synthesized samples, (a) Nano-KFO/NF and (b) PKFO/NF, respectively.

2. Theoretical Section

2.1 Computation Details

The generalized gradient approximation (GGA) with the Perdew-Burke-Ernzerhof exchange-correlation functional is used to perform all the density functional theory (DFT) computations within the frame of Vienna *ab initio* simulation package (VASP).[2,3,4] The projector-augmented plane wave (PAW) is employed to describe the electron-

ion interactions,[5,6] and a 450-eV cutoff for the plane-wave basis set. Moreover, the dispersion interactions are considered by using a semi-empirical van der Waals (vdW) correction proposed by Grimme (DFT-D2).[7,8] Here, 5×5×5 and 3×3×1 Monkhorst-Pack grid *k*-points are adopted to optimize the powder and slab structures of KFO, respectively. In this work, the convergence threshold is set as 10^{-4} eV in energy and 0.02 eV/Å in force. For all the calculations of slab models, the symmetrization is switched off and the dipolar correction is included.

2.2 The Powder and Slab Structures for the KFO System

The KFO is a new 3D open-framework ferrite (Fig. S6), which belongs to the trigonal space group $P\bar{3}1m$, and the optimized unit cell parameters are a = b = 5.006 Å and c = 6.633 Å, all of which are very close to the corresponding experimental values (a = b = 5.155 and c = 6.902 Å).[9] Furthermore, we have performed the correlative DFT computations by constructing the theoretical model to simulate the Fe-O surface, which corresponds to the index (001) surface realized by our experiment. Specifically, the exposed surface of Fe-O layer can be obtained by cleaving the powder structure through the corresponding (001) plane, and can be modeled by the corresponding slab (Fig. S6b). During the computational process, the outermost Fe-O layer in the theoretical slab model is fully relaxed without any symmetry or direction restrictions, while the remaining atoms are kept frozen.

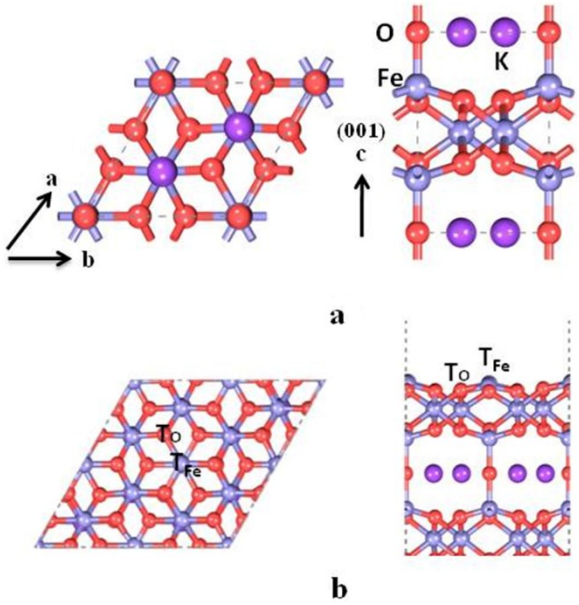

Fig. S6. The top and side views of the (a) powder structure and (b) slab model corresponding to the (001) surface for the KFO system.

2.3 The Theoretical Evaluation of Catalytic Activity for the Hydrogen Evolution Reaction (HER) and Oxygen Evolution Reaction (OER) on the KFO System

In the water splitting process, the dissociation of water may lead to several surface intermediates including OH, O, and H species. The reactions connecting the different states of the surface can be written such as:

$$H_2O + * \leftrightarrow OH^* + e^- + H^+ \quad (1)$$

$$OH^* + * \leftrightarrow O^* + e^- + H^+ \quad (2)$$

$$* + e^- + H^+ \leftrightarrow H^* \quad (3)$$

Where * denotes a free site on the surface, e^- is an electron in the electrode, and H^+ denotes a proton.

In this study we initially explore the adsorption of OH, O, and H species to get the stable surface phase by using the following correlative formulas. The adsorption free energy for OH, O and H is calculated by the following equation:

$$\Delta G = \Delta E + \Delta ZPE - T\Delta S + \Delta G_{pH} \quad (4)$$

Where the reaction energy, ΔE, which refers here to the change in the electronic energy between the products and the reactants, is calculated directly from the DFT

results. For the eqns (1) and (2), Δ*E* can be computed via the formula Δ*E* = E_{ads} + n/2 E_{H_2} - E_{H_2O}, where n is 1 and 2 for eqn (1) and eqn (2), respectively. For eqn (3), Δ*E* can be computed by the formula Δ*E* = E_{ads} - 1/2E_{H_2}.Note that H_2O in the gas phase is also used as reference state, where the entropy for gas phase water is computed at 0.035 bars, since it is the equilibrium pressure in contact with liquid water at 298 K. The difference in zero-point energies, ΔZPE, and the change in entropy Δ*S* are determined by using DFT-calculated vibrational frequencies and standard tables for the gas-phase molecule. Note that for all the above details, we follow the schemes proposed by Nørskov *et al*.[10] ΔG_{pH} = -kTln10×pH is the contribution of the pH in solutions different from 0.[11]

2.3.1 Computational Details on HER

Hydrogen evolution reaction (HER) is one of the half reactions involved in the water-splitting reaction. Subsequently, we construct the structuralmodel of OH-covered (001) surface with the adsorption of OH at the Fe atom of the outmost layer to further investigate the HER catalytic activity of KFO in alkaline condition. The HER catalytic activities for the OH-covered (001) surface areevaluated by computing the ΔG_{H^*} values of possible catalytic sites according to the equation $\Delta G_{H^*} = \Delta E_{H^*}$ + ΔZPE - *T*Δ*S* + kTln10 × pH. Our computed results reveal that on the OH-covered KFO surface, the obtained ΔG_{H^*} values at the Fe site (T_{Fe}) and O site (T_O) in OH group are 0.37 and 2.12 eV, respectively (Figure 4a). Clearly, the O site can serve as the most active site, and the (001) surface of KFO can exhibit high HER catalytic activity.

2.3.2 Computational Details on OER

The oxygen evolution reaction (OER) is another half-reaction of the electrocatalystic water splitting. Usually, the scheme developed by Nørskov*et al*. can be employed to gain an insight into the OER, where the OER is assumed to involve four elementary reaction steps and each step involves electron transfer accompanied by proton expulsion.[12,13,14] For the total reaction $H_2O \rightarrow 1/2O_2 + H_2$, the free-energy

change is fixed at the experimental value of 2.46 eV per water molecule. When forming one molecule of O_2 in the reaction step, the reaction free energy can be expressed as $\Delta G_{(2H2O\rightarrow O2+2H2)} = 4.92$ eV $= E_{O2} + 2E_{H2} - 2E_{H2O} + (\Delta ZPE - T\Delta S)_{(2H2O\rightarrow O2+2H2)}$. In view of the effect of pH value, the free energy of the OER is computed by the equation $\Delta G = \Delta E + \Delta ZPE - T\Delta S + \Delta G_{pH}$. The contribution of pH value in solutions different from 0 can be considered by using $\Delta G_{pH} = -kT\ln10\cdot pH$ term, where T is the temperature and k is the Boltzmann constant. The value of ΔE is obtained by the computation of geometrical structures. The values of ΔZPE and ΔS are determined by employing the computed vibrational frequencies and standard tables for the reactants and products in the gas phase.[14] The entropy for the adsorbed atoms/molecules at the surface-active site are assumed to be zero. The temperature dependence of the enthalpy is neglected in the calculations. Moreover, an external bias U is imposed on each step by including a $-eU$ term in the computation of reaction free energy. Consequently, the reaction free energy of each step can be expressed as follows:

$$\Delta G_A = E(HO^*) - E(^*) - E_{H2O} + 1/2E_{H2} + (\Delta ZPE - T\Delta S)_A - kT\ln10\cdot pH - eU \quad (5)$$

$$\Delta G_B = E(O^*) - E(HO^*) + 1/2E_{H2} + (\Delta ZPE - T\Delta S)_B - kT\ln10\cdot pH - eU \quad (6)$$

$$\Delta G_C = E(HOO^*) - E(O^*) - E_{H2O} + 1/2E_{H2} + (\Delta ZPE - T\Delta S)_C - kT\ln10\cdot pH - eU \quad (7)$$

$$\Delta G_D = E(^*) - E(HOO^*) + E_{O2} + 1/2E_{H2} + (\Delta ZPE - T\Delta S)_D - kT\ln10\cdot pH - eU \quad (8)$$

Here $E(^*)$, $E(HO^*)$, $E(O^*)$, and $E(HOO^*)$ are the computed DFT energies of the pure surface and the adsorbed surfaces with HO*, O*,and HOO*, respectively. E_{H2O}, E_{H2} and E_{O2} are the computed energies for the sole H_2O, H_2 and O_2 molecules, respectively. As a result, the reaction overpotential can be obtained by evaluating the difference between the minimum voltage needed for the OER and the corresponding voltage needed for changing all the free-energy steps into downhill.

Table S1. A properties comparison of various electrocatalysts for hydrogen evolution reaction (HER).

Catalysts (HER)	Overpotential at 10 mA cm^{-2} (mV)	Overpotential at 100 mA cm^{-2} (mV)	Overpotential at 1000 mA cm^{-2} (mV)	Overpotential at 2000 mA cm^{-2} (mV)	Reference
Nano-KFO/NF	**109**	**208**	**302**	**343**	**This work**
Pt/C/NF	**67**	**225**	**739** (500 mA cm^{-2})	——	**This work**
Co/CNFs	190	——	——	——	[15]
CoFeZr oxides/NF	104	≈230	——	——	[16]
CoFe@NiFe/NF	240	≈340	——	——	[17]
Co_9O_8/Ni_3S_2/NF	128	≈230	——	——	[18]
MoS_2-NiS_2/NGF	172	——	——	——	[19]
Ni doped graphitic carbon (NGC)	220	≈580	——	——	[20]
$NiOOH/Ni(OH)_2$	147	——	——	——	[21]
CoMoP nanosheet arrays@NF	173	≈305	——	——	[22]
Ni_3FeN/r-GO	94	≈200	——	——	[23]
P-Co_3O_4/NF	97	——	——	——	[24]
CoP@3D Ti_3C_2-MXene	168	——	——	——	[25]
$Co/Co_2Mo_3O_8$/NF	25	≈210	——	——	[26]
P-doped CoNiS/NF	187.4	≈220	≈240 (500 $mAcm^{-2}$)	——	[27]
N-doped Ni_3S_2 nanosheets	155	≈320	——	——	[28]
RuO_2/NiO/NF	22	≈100	——	——	[29]
Ni_2P-Ni_3S_2 HNAs/NF	80	≈180	——	——	[30]
Sn-Ni_3S_2/NF	35	170	570	——	[1]
Fe-Ni_2P	214 (50 mA cm^{-2})	≈260	——	——	[31]

Ni_3S_2-NGQDs/NF	218	——	——	——	[32]
NiFe/$Ni(OH)_2$/NiAl	78	——	——	——	[33]
MoP/Ni_2P/NF	75	——	——	——	[34]
Mo-Ni_3S_2 nano-rods	——	278	——	——	[35]
g-CN@G MMs	219	——	——	——	[36]
Chemicallyexfoliated MoS_2/carbon cloth	191	——	——	——	[37]
1T-2H N-$MoSe_2$/graphene	98	——	——	——	[38]
N(P)-doped 304-type stainless steel mesh	230	——	——	——	[39]
Cu@CoS_x/Cu Foam	134	267	——	——	[40]
CoFePO/NF	87.5	≈250	——	——	[41]
N-Ni_3S_2/ NF	110	≈250	——	——	[42]
$W(CO)_6$@MAF-6	51	——	——	——	[43]
$NiCo_2S_4$ nanowire arrays	210	——	——	——	[44]

Table S2. A properties comparison of various electrocatalysts for oxygen evolution reaction (OER).

Catalyst (**OER**)	Overpotential at 10 mA cm^{-2} (mV)	Overpotential at 100 mA cm^{-2} (mV)	Overpotential at 1000 mA cm^{-2} (mV)	Overpotential at 2000 mA cm^{-2} (mV)	Reference
Nano-KFO/NF	**241**	**308**	**375**	**421**	**This work**
RuO_2/NF	**257**	**348**	**731**	——	**This work**
Co/CNFs	320	≈450	——	——	[15]
NiFe−LDH/Fe−N−C	310	——	——	——	[45]
CoFePO/NF	274.5	≈410	——	——	[41]
Co_9O_8/Ni_3S_2/NF	227	≈280	——	——	[18]
P-doped Co−Ni−S/NF	292.2	≈300	≈440 (500 mA cm^{-2})	——	[27]
CoP@3D Ti_3C_2-MXene	298	≈370	——	——	[25]
CoMoO nanosheet arrays@NF	270	330	——	——	[22]
Ni_3FeN/r-GO	270	≈320	——	——	[23]
P-Co_3O_4/NF	260 (20 mA cm^{-2})	——	——	——	[24]
RuO_2/NiO/NF	250	≈330	——	——	[29]
Ni_2P-Ni_3S_2 HNAs/NF	210	≈340	——	——	[30]
Fe-Ni_2P	230 (50 mA cm^{-2})	≈250	——	——	[31]
Ni_3S_2-NGQDs/NF	216	≈400	——	——	[32]
NiFe/$Ni(OH)_2$/NiAl	246	315	——	——	[33]
MoP/Ni_2P/NF	——	365	——	——	[34]
N(P)-doped 304-type stainless steel mesh	278	——	——	——	[39]
Cu@CoS_x/Cu Foam	160	310	——	——	[40]
N-Ni_3S_2/NF	——	330	——	——	[42]

$NiCo_2S_4$ nanowire arrays	260	——	——	——	[44]
NiFeOOH	——	259	286	——	[46]
$LaNiO_3$	189	≈300	——	——	[47]
$NiPS_3$	294	351	——	——	[48]
amorphous cobalt phyllosilicate (ACP)	367	——	——	——	[49]
CoS_x	≈390	≈500	——	——	[50]
$CeO_x/NiFeO_x$	300 (20 mA cm^{-2})	——	——	——	[51]
FeCoP allay	252	——	——	——	[52]
Ni-Fe-OH@Ni_3S_2/NF	——	≈270	469	——	[53]
Fe-NiSe/NF	233	275	——	——	[54]
Fe-Ni_3S_2/FeNi	282	≈470	——	——	[55]
$Co_{2.25}Cr_{0.75}O_4$	≈350	——	——	——	[56]
N-$(Ni,Fe)_3S_2$/NF	167	≈200	——	——	[57]
Co_3O_4@Ni_3S_2/NF	260 (20 mA cm^{-2})	≈520	——	——	[58]
Sn-Ni_3S_2/NF	——	270	580	——	[1]
Ni_3Fe/N-C sheets	390	——	——	——	[59]
CP/CTs/Co-S	306	——	——	——	[60]
NiCoP	280	——	——	——	[61]

Table S3. A properties comparison of various electrocatalysts for overall water splitting (OWS).

Catalyst (**OWS**)	Voltage at 10 mA cm^{-2} (V)	Voltage at 100 mA cm^{-2} (V)	Voltage at 1000 mA cm^{-2} (V)	Reference
Nano-KFO/NF	**1.59**	**1.73**	**1.96**	**This work**
Pt/C/NF‖RuO_2/NF	**1.54**	**1.81**	——	**This work**
Co/CNFs	1.60	——	——	[15]
CoFeZr oxides/NF	1.63	≈1.80	——	[16]
CoFe@NiFe/NF	1.59	——	——	[17]
Co_9S_8/Ni_3S_2/NF	1.64	——	——	[18]
MoS_2-NiS_2/NGF	1.64	——	——	[19]
Ni doped graphitic carbon (NGC)	1.64	——	——	[20]
CoMoO nanosheet arrays@NF	1.68	≈1.88	——	[22]
Ni_3FeN/r-GO	1.60	≈1.96	——	[23]
P-Co_3O_4/NF	1.63	——	——	[24]
CoP@3D Ti_3C_2-MXene	1.57	≈1.70	——	[25]
P-doped Co-Ni-S/NF	1.60	——	——	[27]
RuO_2/NiO/NF	1.50	——	——	[29]
Ni_2P-Ni_3S_2 HNAs/NF	1.50	1.62	——	[30]
Fe-Ni_2P	1.49	≈1.73	——	[31]
Ni_3S_2-NGQDs/NF	1.58	——	——	[32]
NiFe/$Ni(OH)_2$/NiAl	1.59	——	——	[33]
MoP/Ni_2P/NF	1.55	——	——	[34]
Mo-Ni_3S_2 nano-rods	1.53	——	——	[35]
N(P)-doped 304-type stainless steel mesh	1.74	——	——	[39]
Cu@CoS_x/Cu Foam	1.50	1.80	——	[40]
CoFePO/NF	1.56	≈1.95	——	[41]
N-Ni_3S_2/ NF	1.48	≈1.83	——	[42]

$NiCo_2S_4$ NW/ NF	1.63	——	——	[44]
NiFeOOH	——	1.49	1.59 (500 mA cm^{-2})	[46]
CP/CTs/Co-S	1.74	——	——	[60]
NiCoP	1.58	≈1.81	——	[61]
$Ni_{1-x}Fe_x$/NC/NF	1.58	——	——	[62]
Ni@NC800/NF	1.60	——	——	[63]
CP@Ni−P	1.63	——	——	[64]
Ni/NiP	1.61	——	——	[65]

3. Reference for the supporting informance

[1] Jian, J.; Yuan, L.; Qi, H.; Sun, X. J.; Zhang, L.; Li, H.; Yuan, H. M.; Feng, S. H. *ACS Appl. Mater. Interfaces,* 2018, **10**, 40568.

[2] Perdew, J. P.; Burke, K.; Ernzerhof, M. *Phys. Rev. Lett.,* 1996, **77**, 3865.

[3] Kresse, G.; Hafner, J. *Phys. Rev. B,* 1993, **47**, 558.

[4] Kresse, G.; Hafner, J. *Phys. Rev. B,* 1994, **49**, 14251.

[5] Blochl, P. E. *Phys. Rev. B,* 1994, **50**, 17953.

[6] Kresse, G.; Joubert, D. *Phys. Rev. B,* 1999, **59**, 1758.

[7] Grimme, S. J. *Comput. Chem.,* 2006, 27, 1787.

[8] Wu, X.; Vargas, M. C.; Nayak, S.; Lotrich, V.; Scoles, G. *J. Chem. Phys.,* 2001, **115**, 8748.

[9] Yuan, H. M.; Li, H.; Zhang, T. S.; Li, G. H.; He, T. M.; Du, F.; Feng, S. H. *J. Mater. Chem. A,* 2018, **6**, 8413.

[10] Nørskov, J. K.; Bligaard, T.; Logadottir, A.; Kitchin, J. R.; Chen, J.; Pandelov, S.; Stimming, U. *J. Electrochem. Soc.,* 2005, **152**, J23.

[11] Nørskov, J. K.; Rossmeisl, J.; Logadottir, A.; Lindqvist, L.; Kitchin, J. R.; Bligaard, T.; Jonsson, H. *J. Phys. Chem. B*, 2004, **108**, 17886.

[12] Rossmeisl, J.; Qu, Z.-W.; Zhu, H.; Kroes, G.-J.; Nørskov, J. K. *J. Electroanal. Chem.*, 2007, **607**, 83.

[13] Valdés, Á.; Qu, Z.-W.; Kroes, G.-J.; Rossmeisl, J.; Nørskov, J. K. *J. Phys. Chem. C*, 2008, **112**, 9872.

[14] Man, I. C.; Su, H.-Y.; Calle-Vallejo, F.; Hansen, H. A.; Martínez, J. I.; N. Inoglu, G.; Kitchin, J.; Jaramillo, T. F.; Nørskov, J. K.; Rossmeisl, J. *ChemCatChem*, 2011, **3**, 1159.

[15] Yang, Z. K.; Zhao, C. M.; Qu, Y. T.; Zhou, H.; Zhou, F. Y.; Wang, J.; Wu, Y.; Li, Y. D. *Adv. Mater.*, 2019, **31**, 1808043.

[16] Huang, L. L.; Chen, D. W.; Luo, G.; Lu, Y. -R.; Chen, C.; Zou, Y. Q.; Dong, C. -L.; Li, Y. F.; Wang, S. Y. *Adv. Mater.*, 2019, 1901439.

[17] Yang, R.; Zhou, Y. M.; Xing, Y. Y.; Li, D.; Jiang, D. L.; Chen, M.; Shi, W. D.; Yuan, S. Q. *Appl. Catal., B,* 2019, **253** 131.

[18] Du, Feng.; Shi, L.; Zhang, Y. T.; Li, T.; Wang, J. L.; Wen, G. H.; Alsaedi, A.; Hayat, T.; Zhou, Y.; Zou, Z. G. *Appl. Catal., B*, 2019, **253**, 246.

[19] Kuang, P. Y.; He, M.; Zou, H. Y.; Yu, J. G.; Fan, K. *Appl. Catal., B,* 2019, **254**, 15.

[20] Zhou, B. H.; Zhang, M. C.; He, W. Y.; Wang, H. M.; Jian, M. Q.; Zhang, Y. Y. *Carbon,* 2019, **150**, 21.

[21] Patil, B.; Satilmis, B.; Khalily, M. A.; Uyar, T.; *ChemSusChem,* 2019, **12**, 1469.

[22] Zhang, Y.; Shao, Q.; Long, S.; Huang, X. Q. *Nano Energy,* 2018, **45**, 448.

[23] Gu, Y. Chen, S.; Ren, J.; Jia, Y.; Chen, C. M.; Komarneni, S.; Yang, D. J.; Yao, X. D. *ACS Nano,* 2018, **12**, 245.

[24] Wang, Z. C.; Liu, H. L.; Ge, R. X.; Ren, X.; Ren, J.; Yang, D. J.; Zhang, L. X.; Sun, X. P. *ACS Catal*., 2018, **8**, 2236.

[25] Xiu, L. Y.; Wang, Z. Y.; Yu, M. Z.; Wu, X. H.; Qiu, J. S. *ACS Nano,* 2018, **12**, 8017.

[26] Zang, M. J.; Xu, N.; Cao, G. X.; Chen, Z. J.; Cui, J.; Gan, L. Y.; Dai, H. B.; Yang, X. F.; Wang, P. *ACS Catal*., 2018, **8**, 5062.

[27] Zhang, F. F.; Ge, Y. C.; Chu, H.; Dong, P.; Baines, R.; Pei, Y.; Ye, M. X.; Shen, J. F. *ACS Appl. Mater. Interfaces,* 2018, **10**, 7087.

[28] Kou, T. Y.; Smart, T.; Yao, B.; Chen, I.; Thota, D.; Ping, Y.; Li, Y. *Adv. Energy Mater*., 2018, **8**, 1703538.

[29] Liu, J. S.; Zheng, Y.; Jiao, Y.; Wang, Z. Y.; Lu, Z. G.; Vasileff, A.; Qiao, S. -Z. *Small,* 2018, **14**, 1704073.

[30] Zeng, L. Y.; Sun, K. A.; Wang, X. B.; Liu, Y. Q.; Pan, Y.; Liu, Z.; Cao, D. W.; Song, Y.; Liu, S. H.; Liu, C. G. *Nano Energy,* 2018, **51**, 26.

[31] Li, Y. J.; Zhang, H. C.; Jiang, M.; Zhang, Q.; He, P. L.; Sun, X. M. *Adv. Funct. Mater*., 2017, **27**, 1702513.

[32] Lv, J. J.; Zhao, J.; Fang, H.; Jiang, L. P.; Li, L. L.; Ma, J.; Zhu, J. J. *Small,* 2017, **13**,1700264.

[33] Niu, S.; Jiang, W. -J.; Tang, T.; Zhang, Y.; Li, J. -H.; Hu J. -S. *Adv. Sci*., 2017, **4**, 1700084.

[34] Du, C. C.; Shang, M. X.; Mao J. X.; Song W. B. *J. Mater. Chem. A*, 2017, **5**, 15940.

[35] Cui, Z.; Ge, Y. C.; Chu, H.; Baines, R.; Dong, P.; Tang, J. H.; Yang, Y.; Ajayan, P. M.; Ye, M. X.; Shen, J. F. *J.Mater.Chem. A*, 2017, **5**, 1595.

[36] Han, Q.; Cheng, Z. H.; Gao, J.; Zhao, Y.; Zhang, Z. P.; Dai, L. M.; Qu, L. T. *Adv. Funct. Mater*., 2017, 1606352.

[37] Chen, Y. -C.; Lu, A. -Y.; Lu, P.; Yang, X. L.; Jiang, C. -M.; Mariano, M.; Kaehr, B.; Lin, O.; Taylor, A.; Sharp, L. D.; Li, L. -J. Chou, S. S.; Tung, V. *Adv. Mater*., 2017, 1703863

[38] Deng, S. J.; Zhong, Y.; Zeng, Y. X.; Wang, Y. D.; Yao, Z. J.; Yang, F.; Lin, S. W.; Wang, X. L.; Lu, X. H.; Xia, X. H.; Tu, J. P. *Adv. Mater*., 2017, 1700748.

[39] Balogun, M. -S.; Qiu, W. T.; Huang, Y. C.; Yang, H.; Xu, R. M.; Zhao, W. X.; Li, G. -R.; Ji, H. B.; Tong, Y. X. *Adv. Mater*., 2017, 1702095.

[40] Liu, Y. P.; Li, Q. J.; Si, R.; Li, G. -D.; Li, W.; Liu, D. -P.; Wang, D. J.; Sun, L.; Zhang, Y.; Zou, X. X. *Adv.Mater*., 2017, **29**, 1606200.

[41] Duan, J. J.; Chen, S.; Vasileff, A.; Qiao, S. Z. *ACS Nano,* 2016, **10**, 8738

[42] Chen, P. Z.; Zhou, T. P.; Zhang, M. X.; Tong, Y.; Zhong, C. A.; Zhang, N.; Zhang, L. D.; Wu, C. Z.; Xie, Y. *Adv.Mater*., 2017, **29**, 1701584.

[43] Xu, Y. T.; Xiao, X. F.; Ye, Z. M.; Zhao, S. L.; Shen, R. G.; He, C. T.; Zhang, J. P.; Li, Y. D.; Chen, X. M. *J. Am. Chem. Soc*., 2017, **139**, 5285.

[44] Sivanantham, A.; Ganesan, P.; Shanmugam, S. *Adv. Funct. Mater*., 2016, **26**, 4661.

[45] Dresp, S.; Luo, F.; Schmack, R.; Kuhl, S.; Gliech, M.; Strasser, P. *Energy Environ. Sci*., 2016, **9**, 2020.

[46] Zhou, H. Q.; Yu, F.; Zhu, Q.; Sun, J. Y.; Qin, F.; Yu, L.; Bao, J. M.; Yu, Y.; Chen, S.; Ren, Z. F. *Energy*

Environ. Sci., 2018, **11**, 2858.

[47] Chen, G.; Zhu, Y. P.; Chen, H. M.; Hu, Z. W.; Hung, S. F.; Ma, N. N.; Dai, J.; Lin, H. J.; Chen, C. T.; Zhou, W. *Adv. Mater.,* 2019, 1900883.

[48] Xue, S.; Chen, L.; Liu, Z. B.; Cheng, H. -M.; Ren, W. C. *ACS Nano,* 2018, **12**, 5297.

[49] Kim, J. S.; Park, I.; Jeong, E. S.; Jin, K.; Seong, W. M.; Yoon, G.; Kim, H.; Kim, B.; Nam, K. T.; Kang, K. *Adv. Mater*., 2017, 1606893.

[50] Fan, K.; Zou, H. Y.; Lu, Y.; Chen, H.; Li, F. S.; Liu, J. X.; Sun, L. C.; Tong, L. P.; Toney, M. F; Sui, M. L; Yu, J. G. *ACS Nano,* 2018, **12**, 12369.

[51] Obata, K.; Takanabe, K. *Angew. Chem.,* 2018, **130**, 1632.

[52] Liu, K. W.; Zhang, C. L.; Sun, Y. D.; Zhang, G. H.; Shen, X. C.; Zou, F.; Zhang, H. C.; Wu, Z. W.; Wegener, E. C.; Taubert, C. J.; Miller, J. T.; Peng, Z. M.; Zhu, Y. *ACS Nano,* 2018, **12**, 158.

[53] Zou, X.; Liu, Y. P.; Li, G. -D.; Wu, Y. Y.; Liu, D. -P.; Li, W.; Li, H. -W.; Wang, D. J.; Zhang, Y.; Zou, X. X. *Adv. Mater*., 2017, 1700404.

[54] Zhao, Q.; Zhong, D. Z.; Liu, L.; Li, D. D.; Hao G. Y.; Li, J. P. *J. Mater. Chem. A*, 2017, **5**,14639.

[55] Yuan, C. -Z.; Sun, Z. -T.; Jiang, Y. -F.; Yang, Z. -K.; Jiang, N.; Zhao, Z. -W.; Qazi, U. Y.; Zhang, W. H.; Xu, A. -W. *Small,* 2017, **13**, 1604161.

[56] Lin, C. C.; McCrory, C. C. L. *ACS Catal*., 2017, **7**, 443.

[57] Gong, Y. Q.; Xu, Z. F.; Pan, H. L.; Lin, Y.; Yang, Z.; Du, X. Q. *J. Mater. Chem. A*, 2018, **6**, 5592.

[58] Jin, Y. S.; Yue, X.; Du, H. Y.; Wang, K.; Huang, S. L.; Shen, P. K. *J. Mater. Chem. A*, 2018, **6**, 5098.

[59] Fu, G. T.; Cui, Z. M.; Chen, Y. F.; Li, Y. T.; Tang, Y. W.; Goodenough, J. B. *Adv. Energy Mater.,* 2017, **7**,1601172.

[60] Wang, J.; Zhong, H. -X.; Wang, Z. -L.; Meng, F. -L.; Zhang, X. -B. *ACS Nano,* 2016, **10**, 2342.

[61] Liang, H. F.; Gandi, A. N.; Anjum, D. H.; Wang, X. B.; Schwingenschlogl, U.; Alshareef, H. N. *Nano Lett.,* 2016, **16**, 7718.

[62] Zhang, X.; Xu, H. M.; Li, X. X.; Li, Y. Y.; Yang, T. B.; Liang, Y. Y. *ACS Catal*., 2016, **6**, 580.

[63] Xu, Y.; Tu, W. G.; Zhang, B. W.; Yin, S. M.; Huang, Y. Z.; Kraft, M; Xu, R. *Adv. Mater*., 2017, **29**, 1605957.

[64] Wang, X. G.; Li, W.; Xiong, D. H.; Petrovykh, D. Y..; Liu, L. F. *Adv. Funct. Mater.,* 2016, **26**, 4067.

[65] Chen, G. F.; Ma, T. Y.; Liu, Z. Q.; Li, N.; Su, Y. Z.; Davey, K.; Qiao, S. Z. *Adv. Funct. Mater*., 2016, **26**, 3314.